ACS Catalysis
RESEARCH ARTICLE
pubs.acs.org/acscatalysis

Stainless Steel As a Catalyst for the Total Deoxygenation of Glycerol and Levulinic Acid in Aqueous Acidic Medium

Domenico Di Mondo,[†] Devipriya Ashok,[†] Fraser Waldie,[†] Nick Schrier,[‡] Michael Morrison,[‡] and Marcel Schlaf*,[†]

[†]Department of Chemistry, University of Guelph, The Guelph-Waterloo Centre for Graduate Work in Chemistry (GWC)^2, 50 Stone Road, East Guelph, Ontario N1G 2W1, Canada

[‡]Laboratory Services Division, University of Guelph, P.O. Box 3650, 95 Stone Road, West Guelph, Ontario N1H 8J7 Canada

S *Supporting Information*

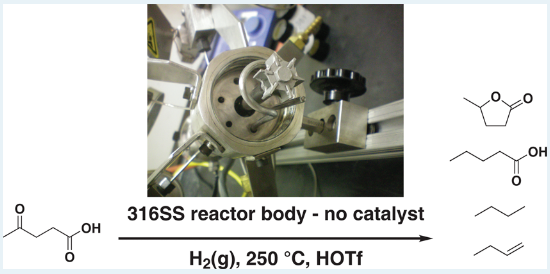

ABSTRACT: Exposing 316 Stainless Steel pressure reactor bodies to an aqueous Brønstedt acidic solution (trifluoromethane sulfonic acid) at elevated temperatures (100−250 °C) under reducing atmosphere (hydrogen gas at 800 psi) leads to the formation of insoluble inorganic precipitates, identified as mixed chromium oxides by scanning electron microscopy X-ray fluorescence (SEM-XRF). A catalytically active metal surface is generated, that is, under these conditions the <100 Å thick chromium oxide layer that normally passivates 316 Stainless Steel (316SS) against corrosion is etched away, and the reactor body itself becomes an active hydrogenation catalyst. The effect is specific to aqueous acidic medium and therefore water-soluble substrates as encountered in biomass conversion, for example, sugar alcohols and levulinic acid, which can be deoxygenated to the corresponding alkanes and alkenes using only a Brønstedt acid and the reactor body as the catalyst. Control experiments in several different 316SS reactors built by different manufacturers from different batches of 316SS as well as inductively coupled plasma optical emission spectroscopy (ICP-OES) and mass spectrometry (ICP-MS) analysis of the chromium oxide precipitates formed and steel samples from the reactor body itself indicate that the catalytic activity is not caused by trace amounts of ruthenium or another hydrogenating metal such as Re, Rh, Ir, Pd, or Pt. The observed catalytic activity scales with the concentration of acid and the addition of 316SS added to the reaction mixture as a powder conclusively establishing 316SS as the active catalyst.

KEYWORDS: stainless steel, catalysis, aqueous medium, hydrogenation, deoxygenation, biomass conversion

INTRODUCTION

A general strategy for the deoxygenation of carbohydrate derived biomass to petrochemicals and fuels is the iterative acid-catalyzed dehydration and metal-catalyzed hydrogenation of the polyhydroxy sugar substrates and their resulting condensation products to ultimately give alkanes. In principle both heterogeneous and homogeneous acid- and metal-catalysts can be employed,[1−9] which by the nature of the process must be both acid- and water-stable, qualities that in the context of classical petrochemistry are unusual for (heterogeneous) hydrogenation catalysts and their supports.[10] In addition (and even in the presence of an acid catalyst), the need to overcome the activation barriers for dehydration of the polyhydroxy substrates generally requires temperatures ≫150 °C.[11] Catalytic deoxygenation reactions are therefore typically carried out in high-pressure hydrogenation reactors made from 316 stainless steel (316SS), an alloy of Fe, Cr (12−20%), Ni (10−14%), Mo (2−3%), Mn (<2%) and in some cases smaller amounts of Si (<1%), P (<0.045%), and S (<0.03%), that is generally considered to be inert and highly corrosion resistant, as it passivates itself through the build-up of a mechanically strongly adherent chromium oxide layer of <100 Å thickness.[12]

There are however isolated reports on the activity of stainless steel as a catalyst, at least one of which is of eminent historical importance: Holzkamp and Ziegler's discovery that traces of Nickel leached from a stainless steel pressure vessel are an active catalyst for the dimerization of ethylene to butane which ultimately led to the development of transition metal based polymerization catalysts.[13,14] Approximately at the same time it was reported that sodium-promoted finely divided stainless steel acts as Fischer−Tropsch catalyst.[15] At more extreme temperatures (500−700 °C) stainless steel can effect the hydrogenolysis of *n*-heptane to C1−C6 hydrocarbons.[16] At even higher temperatures (∼ 800 °C) 316SS reactor walls have been shown to affect the decomposition of methane to hydrogen and coke and also play a role in the mechanism of coke formation in the pyrolysis of octanoic acid.[17,18] It has also been established that in supercritical carbon dioxide 316SS catalyzes the oxidation of olefins with molecular oxygen and sacrificial aldehyde.[19] Hao et al. have demonstrated the activity of a stainless steel reactor wall in the catalytic oxidation of cyclohexane to cyclohexanol and cyclohexanone. More important in the present context, Arai and co-workers reported that the hydrogenation of

Received: February 1, 2011
Revised: February 16, 2011
Published: March 03, 2011

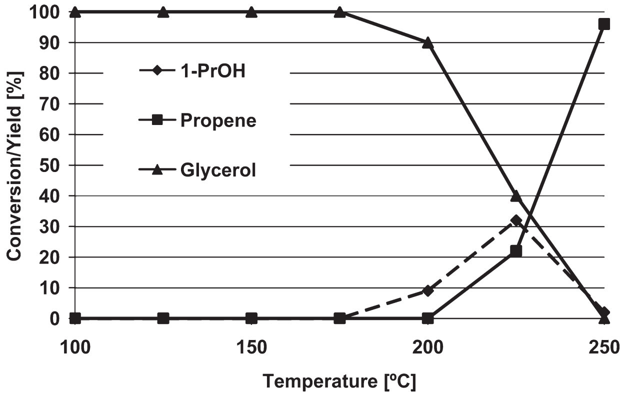

Figure 1. Deoxygenation of glycerol in water catalyzed by HOTf/316SS as a function of temperature. Reaction conditions: glycerol [500 mmol/L], HOTf [40 mmol/L], 800 psi $H_2(g)$ (initial pressure at ambient temperature), dimethylsulfone (ISTD) [100 mmol/L], reaction time = 24 h.

2-butyne-1,4-diol in supercritical carbon dioxide, ethanol, or water can also be catalyzed by a stainless steel reactor wall;[20,21] however, no control experiments were carried out that would have unambiguously established that the reaction was in fact not mediated by traces of metal deposits from previous reactions carried out in the reactor.

We recently described the use of the acid-, water-, and high-temperature-stable system HOTf/[Ru(H_2O)$_3$(4′-phenyl-terpyridine)](OTf)$_2$ (OTf^- = trifluoromethylsulfonate, "*triflate*") as a homogeneous catalyst for the total deoxygenation of glycerol in sulfolane and also in aqueous medium.[22] Subsequently we explored the potential applicability of this and other similar homogeneous catalyst systems to other substrates, notably the C4 and C5 building blocks (1,4-anhydro)-erythritol and levulinic acid,[23,24] as the (possibly selective) deoxygenation of both these substrates to tetrahydrofuran (THF) and pentanoic acid, respectively, is of economic and industrial interest, for the latter because of the use of ethyl, propyl, or pentyl pentanoate (valerate) as a fuel or fuel additive.[25−32] Carrying out control reactions with these substrates, we discovered that at temperatures >175 °C and in HOTf/water as the reaction medium—and in water only !—the 316SS used to construct the body of the hydrogenation reactor becomes activated, acting as a hydrogenation catalyst for the total deoxygenation of the title substrates. Here we present what we believe to be the first detailed study on the activation and use of 316SS as a hydrogenation catalyst in aqueous acidic medium as a function of the acid concentration and temperature using the deoxygenation of the water-soluble substrates glycerol and levulinic acid as example reactions and compare the activity of 316SS to typical and commercially available Ru/C hydrogenation catalysts.

RESULTS

Catalytic Deoxygenation of Glycerol by 316SS in Aqueous Acidic Medium. After discovering that 316SS was in fact acting as a hydrogenation catalyst for sugar polyalcohol derived carbonyl and alkene substrates, if the reaction medium is pure water and HOTf is present as an activator (vide infra for the detailed experimental validation of 316SS as a catalyst and a possible activation mechanism), we reinvestigated the deoxygenation of glycerol under these conditions as a function of temperature and acid concentration in detail. Figures 1 and 2 and Table 1 (entries 1−7) summarize the results of this study. At temperatures >175 °C and at a constant acid concentration of 40 mmol/L, the reaction starts to consume $H_2(g)$ generating *n*-propanol and ultimately propene via the previously established and discussed pathway shown in Scheme 1.[22] After 24 h reaction time a maximum yield of 32% *n*-propanol (by quantitative GC against 100 mmol/L dimethyl sulfone as an internal standard) is achieved at 225 °C. Small amounts of *i*-propanol are also present, which under the aqueous reaction conditions must arise from Markovnikov readdition of water to propene, which is detectable by GC-MS in gas samples taken from the headspace of the reactor at $T > 200$ °C after 2 h. At 250 °C no GC-analyzable products remain in the aqueous phase after 24 h, only propene is detectable in the gas phase (by TCD-micro-GC and GC-MS against an authentic standard). HPLC analysis (RI detector) of the remaining solution using a sulfonated polystyrene resin column with 0.01n H_2SO_4 as the mobile phase excludes the presence of any other higher molecular weight condensation products.[33] Figure 2 shows the liquid product distribution obtained as a function of acid concentration at 250 °C. At this temperature the reactions give complete conversion of glycerol after 5 h as indicated by GC analysis, that is, do not require the long 24 h reaction times used in the initial temperature series (Figure 1). They show decreasing alcohol concentration with increasing acid concentration with no 1-propanol remaining with the highest acid concentration. Again no other GC or HPLC detectable products remain in the reaction solution and analysis of gas samples taken from the headspace of the reactor by micro-GC-TCD show propene as the product.[34]

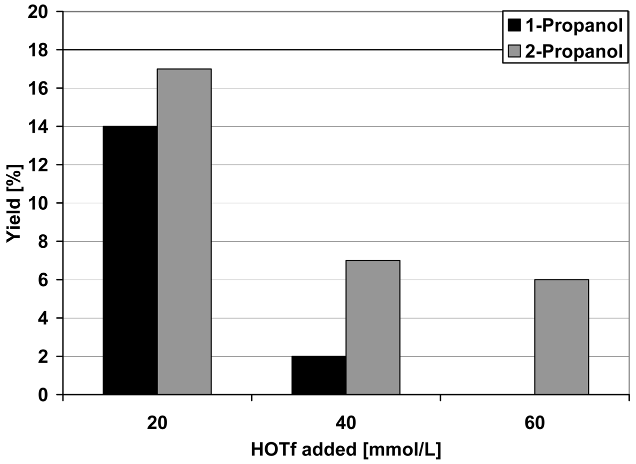

Figure 2. Influence on the amount of HOTf acid added on the activity of 316SS in the deoxygenation of glycerol in water. Reaction conditions: glycerol [500 mmol/L], 800 psi $H_2(g)$ (initial pressure at ambient temperature), dimethylsulfone (ISTD) [100 mmol/L], reaction time = 5 h.

A control reaction with glycerol in sulfolane rather than water (entry 9, Table 1) resulted in only marginal $H_2(g)$ uptake, no conversion to GC-analyzable products, and decomposition of the substrate as indicated by formation of a thick oily brown residue in the reaction solution, while the same reaction in sulfolane, but in the presence of the homogeneous ruthenium catalyst [Ru(H_2O)$_3$(4′-phenyl-terpyridine)](OTf)$_2$ also gave full conversion. These reactions confirm the activity of the ruthenium catalyst in sulfolane as previously reported, but also suggest that our earlier results of glycerol deoxygenation with this catalyst in water should be reinterpreted as representing an overlay of both ruthenium catalyst and 316SS activity.[22,35] A further control reaction without HOTf added did not give any $H_2(g)$ uptake (entry 8, Table 1), but full recovery of the glycerol substrate with no GC-MS identifiable product in the gas headspace of the reactor. Finally a control reaction in water with acid but without the addition of the internal

Table 1. Deoxygenation of Glycerol in Water Catalyzed by HOTf/316SS As a Function of Temperature[a]

entry	T [°C]	solvent/acid/cat.	H_2 uptake [psi]	glycerol [% recovery][b]	*n*-propanol [% yield][b]	*i*-propanol [% yield][b]	propene [% yield][b,c]
1	100	water	2	100	0	trace	0
2	125	water	3	100	0	trace	0
3	150	water	8	100	0	trace	0
4	175	water	10	100	0	trace	0
5	200	water	25	90	8	2	0
6	225	water	98	40	32	6	22
7	250	water	125	0	2	2	96
8	250	water/no acid	0	100	0	0	0
9	250	sulfolane	11	0	0	0	0
10	250	sulfolane/Ru-cat.[d]	97	0	0	0	100

[a] Reaction conditions: glycerol [500 mmol/L], HOTf [40 mmol/L], 800 psi H_2(g) (initial pressure at ambient temperature), dimethylsulfone (ISTD) [100 mmol/L], time =24 h. Nominal reactor volume 50 mL, solution volume 25 mL. [b] By quantitative GC against internal standard dimethylsulfone. [c] Identified in gas sample from reactor headspace by micro-GC (TCD) and GC-MS against an authentic sample; yield by mass-balance. [d] $[Ru(H_2O)_3(4'\text{-phenyl-terpyridine})](OTf)_2$ [2.5 mmol/L = 0.5 mol %].

Scheme 1. Reaction Pathway for the Deoxygenation of Glycerol to Propene

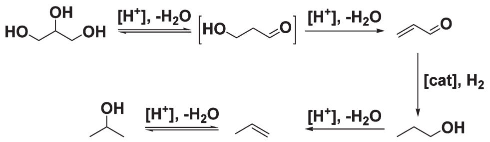

GC standard (ISTD) dimethylsulfone gave the same results, that is, complete conversion of glycerol at 250 °C, establishing that the ISTD plays no role in the observed catalytic activity.

In analogy to our earlier work with $[Ru(H_2O)_3(4'\text{-phenyl-terpyridine})](OTf)_2$ in sulfolane and the deoxygenation of glycerol discussed above,[22] we also reacted 1,2-hexanediol under the same reaction conditions as entry 7, Table 1 (i.e., water and HOTf) giving complete conversion of the substrate and formation of a hexane layer (identified by ^1H NMR, GC, and GC-MS against an authentic sample) floating above the aqueous reaction solution. In a preliminary attempt to extend the observed activity of 316SS to higher sugar alcohols, reaction of 1,4-anhydroerythritol (AHE) leads to a H_2(g) uptake of 71 psi, 47% recovery of the AHE, and the identification of butene and butane in the gas phase headspace of the reactor by GC-MS against an authentic sample of butane. As with glycerol a control reaction in sulfolane rather than water led to decomposition and polymerization with no H_2(g) uptake.

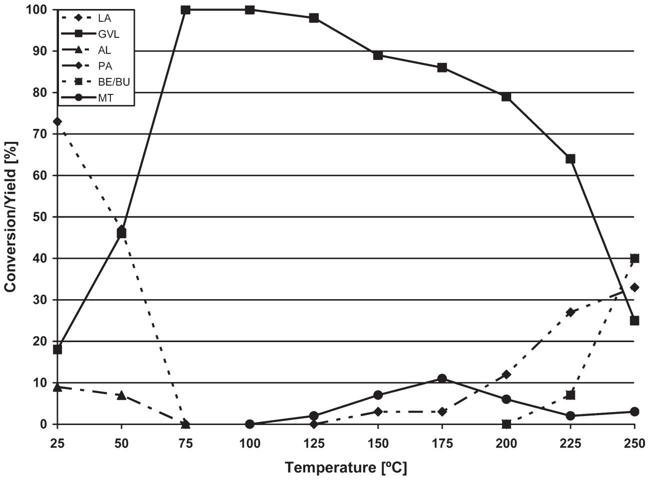

Figure 3. Deoxygenation of levulinic acid in water catalyzed by HOTf/316SS as a function of temperature. LA = levulinic acid; GVL = γ-Valerolactone; AL = α-Angelicalactone, PA = Pentanoic Acid; BE/BU = 1-butene/butane (yield inferred by mass balance); MT = 2-Methyl-tetrahydrofuran. Reaction conditions: LA [500 mmol/L], HOTf [40 mmol/L], 800 psi H_2(g) (initial pressure at ambient temperature), dimethylsulfone (ISTD) [100 mmol/L], time = 24 h.

Application of 316SS As a Catalyst for the Deoxygenation of Levulinic Acid. The results of the deoxygenation of levulinic acid by the 316SS/HOTf system in aqueous medium as a function of temperature are summarized in Figure 3 and Table 2. As the graphs and numerical data show levulinic acid (LA) is highly reactive toward catalytic hydrogenation to γ-valerolactone (GVL) by 316SS even at low temperature reflecting the high enthalpic and entropic driving force of this long established reaction,[36,37] that has recently attracted renewed attention.[7,31,32,38−43] The presence of α-angelicalactone (AL) in the reaction mixture (by GC/GC-MS) at low temperatures suggests that for this first reaction step two pathways may be operating in parallel. Either LA is hydrogenated first and then cyclizes to GVL or cyclization to AL via the acid enol occurs first followed by hydrogenation. In either case GVL is the dominant reaction product after 24 h at temperatures up to 225 °C. With increasing temperature increasing amounts of the secondary hydrogenation products pentanoic acid (PA) and 2-methyl-tetrahydrofuran (MT) appear with the conceivable pathways of the reaction cascade illustrated in Scheme 2.[9,32] The detection of both PA and MT again suggests two parallel reaction pathways from GVL to each of these products. Only trace amounts of 1-pentanol (PO) to a maximum of 2% yield (entry 8, Table 2) were detected, but above 200 °C, the mass balance obtained by quantitative GC-analysis of the liquid phase of the reaction is increasingly deficient. In analogy to the glycerol and 1,2-hexanediol deoxygenation reactions, we therefore hypothesized that total deoxygenation to *n*-pentane had taken place; however, no phase separation of an alkane layer was observed in the reaction mixtures, which we initially attributed to the lower boiling point of *n*-pentane (PE) (bp 35 °C vs bp 69 °C for *n*-hexane) preventing its isolation as a liquid product upon venting the pressurized reactor at the end of the reaction even with cooling of the reactor body with an ice-bath. GC-MS analysis of a sample taken from the gas phase headspace of the reactor before venting subsequently suggested the presence of

Table 2. Deoxygenation of Levulinic Acid in Water Catalyzed by HOTf/316SS As a Function of Temperature[a]

entry	*T* [°C]	levulinic acid [% recovery][b]	angelicalactone [% yield][b]	γ-valerolactone [% yield][b]	pentanoic acid [% yield][b]	1-pentanol [% yield][b]	2-methyl-THF [% yield][b]	1-butene/butane [% yield][b,c]
1	25	73	9	18	0	0	0	0
2	50	47	7	46	0	0	0	0
3	75	0	0	100	0	0	0	0
4	100	0	0	100	0	0	0	0
5	125	0	0	98	0	0	2	0
6	150	0	0	89	3	0	7	0
7	175	0	0	86	3	0	11	0
8	200	0	0	79	12	2	6	0
9	225	0	0	64	27	0	2	7
10	250	0	0	24	33	0	3	40
11[d]	250	18	0	68	10	0	0	4

[a] Reaction conditions: Levulinic acid [500 mmol/L], HOTf [40 mmol/L], 800 psi $H_2(g)$ (initial pressure at ambient temperature), dimethylsulfone (ISTD) [100 mmol/L], in water, time =24 h. Nominal reactor volume 50 mL, solution volume 25 mL. [b] By quantitative GC against internal standard dimethylsulfone. [c] Identified in headspace by GC-MS and TCD-micro-GC against authentic standards, yield inferred by mass-balance. [d] No acid added.

Scheme 2. Reaction Cascade for the Deoxygenation of Levulinic Acid to Pentanoic Acid, Pentane, and 1-Butane/Butane under Aqueous Acidic Conditions[a]

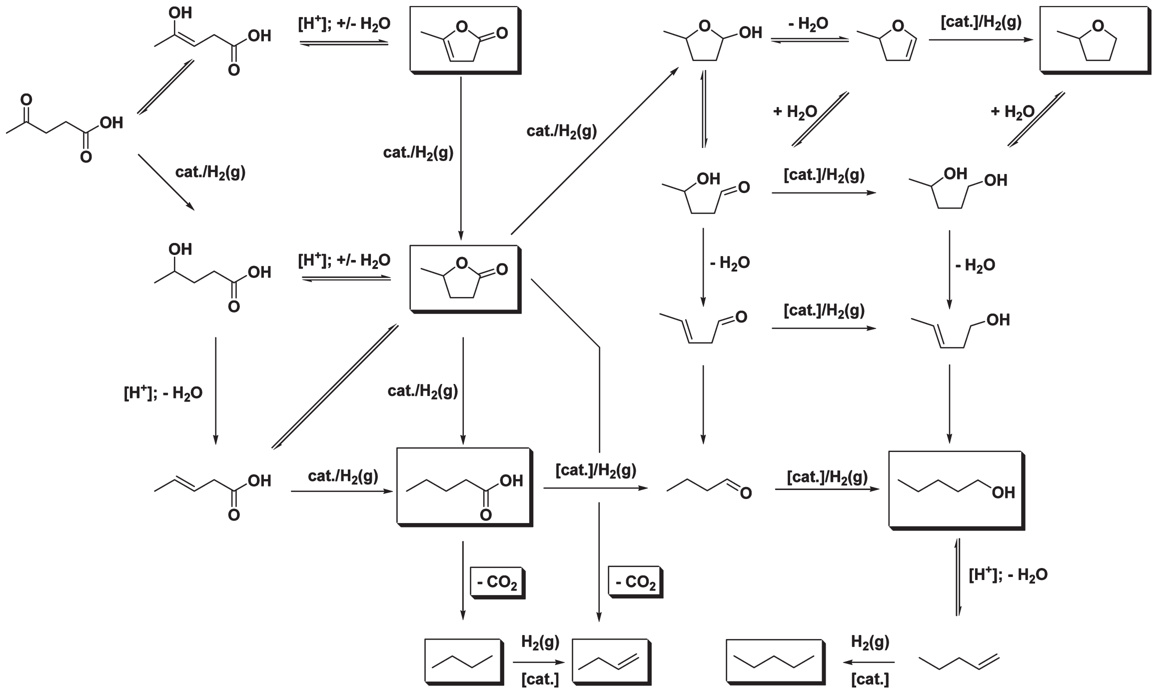

[a] Products and intermediates in boxes were identified by GC-FID/GC-MS/micro-GC-TCD against authentic samples or by their MS fragmentation pattern against a database match.

an alkene, possibly 1-pentene as a product.[44] However, subsequent analysis of samples from the reactor headspace by micro-GC (TCD detector against authentic gas standards of 1000 ppm ethylene/ethane, propene/propane, 1-butene/butane, 1-pentene/pentane, and 1-hexene/hexane in helium revealed the presence of CO_2 and an approximate 1:8 ratio of 1-butene (BE) and butane (BU) but no pentene (PT) or pentane (PE),[45] indicating that the 316SS/HOTf catalyst system not only mediated the hydrogenation of LA to GVL, but also the decarboxylation of GVL and/or PA to 1-butene and/or butane according to the pathways shown in Scheme 2.[46]

At 250 °C the hydrogenation of LA to GVL (68% yield) and smaller amounts of PA (10%) and 1-butene/butane (4%) also proceeds in the absence of added HOTf (Entry 11, Table 2), that is, the intrinsic Brønstedt acidity of the substrate itself appears to be sufficient to activate the reactor body. As with the glycerol deoxygenation, a control reaction in sulfolane rather than water at 250 °C with 40 mmol/L HOTf added as the activator acid resulted in only marginal $H_2(g)$ uptake by the reaction, no GC-analyzable reaction products and the formation of a viscous brown organic residue in the reactor, which we interpret as the product of a nonspecific acid-catalyzed aldol condensation and polymerization of LA with itself, possibly via AL.

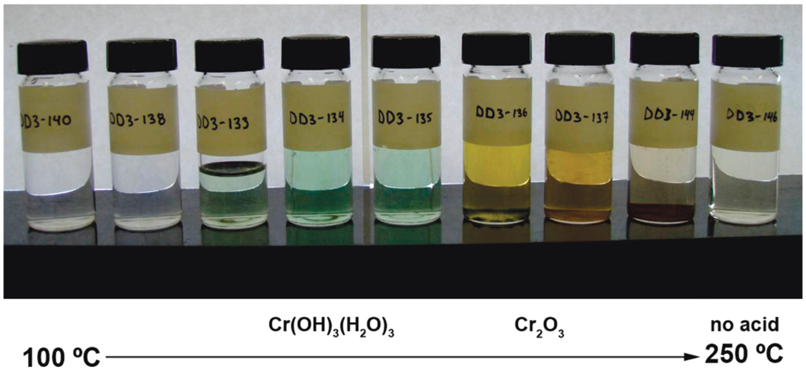

Figure 4. Appearance of the reaction solutions and inorganic precipitates obtained in the deoxygenation of glycerol in water as a function of temperature in the reactions of Table 1/Figure 1. The colorless solution in the vial on the extreme right is the control reaction (entry 8, Table 1) showing no formation of a precipitate and complete recovery of glycerol.

Catalyst Characterization and Validation of Reactor Body as the Catalyst. Following the realization that in aqueous medium the 316SS reactors achieved complete deoxygenation of water-soluble substrates without addition of an actual catalyst, we initially hypothesized that the observed activity was caused by ruthenium metal deposited on the reactor surfaces during the course of several hundred reactions carried out with a variety of homogeneous ruthenium catalysts.[47] However, complete disassembly, sandblasting, and machine polishing of all exposed surfaces of both 50 mL Autoclave Engineers mini-reactors used in the series of experiments gave the same results upon repeating the experiments in the reassembled reactors.[48] Carrying out the same reactions on a larger scale (100 mL reaction solutions) in two 316SS reactors (500 and 600 mL, manufactured by Parr Instruments), whose surfaces had also been machine polished, again gave the same results, that is, complete conversion of glycerol to propene at 250 °C in aqueous acidic medium. Also the surfaces of one of the two reactors (500 mL) had never been exposed to ruthenium or any other hydrogenating metal, that is, Re, Pd, Pt, Rh, or Ir.

Common to all reactions carried out in aqueous acidic medium in the reactors is the formation of an inorganic insoluble precipitate the color and amount of which varies with the reaction temperature as shown in Figure 4 (samples obtained from glycerol deoxygenation reactions). The solution in the vial on the extreme right is that of the control reaction carried out in the absence of acid leading to full recovery of the glycerol substrates (cf. entry 8, Table 1) and did not result in the formation of inorganic insoluble precipitates. Control reactions in the presence of acid but absence of glycerol also result in the formation of inorganic insoluble precipitates.

Scanning electron microscopy X-ray fluorescence (SEM-XRF) analysis (Figure 5) of the green to yellow-brownish precipitates revealed them to be composed in part of chromium oxides along with the other metals and trace elements expected to be present in stainless steel.[49] In addition, fluorine was identified originating from the HOTf present. The presence of dissolved chromium species even in acidic reaction solutions that do not show the formation of a precipitate is further proven by the addition of a few drops of NaOH leading to the formation of a characteristic voluminous green precipitate of $Cr(OH)_3$ (Figure 6),[50] which is, however, not observed from reaction solutions obtained from glycerol deoxygenation reactions carried out at $T < 125$ °C. Qualitatively the amount of $Cr(OH)_3$ formed by addition of base increases with increasing reaction temperature, but is always small in relation to the mass the reactor ($\ll 50$ mg in each case), that is, was not anticipated to jeopardize the integrity of the pressure vessel even over the hundreds of experiments carried out with these reactors. For reactions carried out at $T > 200$ °C, precipitates (probably of mixed $Cr^{III/IV}$ oxides) of increasingly dark yellow to brown are present prior to the addition of NaOH (right side of Figure 4).

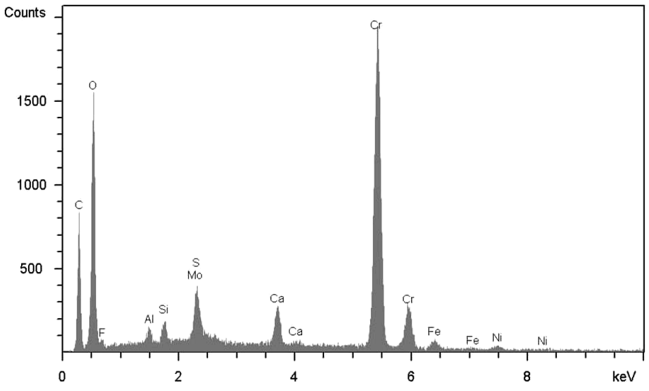

Figure 5. SEM-XRF spectrum of a typical green precipitate isolated from a glycerol deoxygenation reaction.

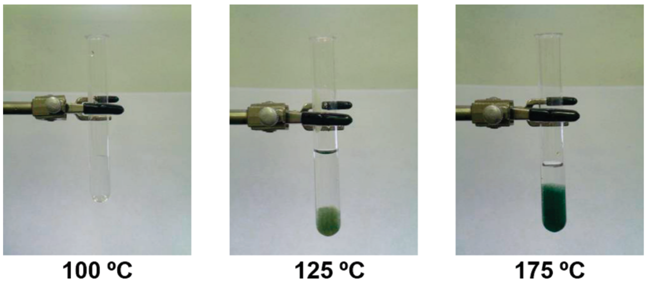

Figure 6. Precipitation of $Cr(OH)_3(H_2O)_3$ from 1:1 (2 + 2 mL) mixtures of water and solutions obtained from glycerol deoxygenation reactions carried out at 100, 125, and 175 °C by addition of 4 drops of 6 M NaOH.

SEM-XRF and wet chemistry analysis are however not suitable for trace analysis of metals, which in the case of ruthenium or other hydrogenating metals could in principle be responsible for the observed catalytic activity even at low concentrations. For example, Buchwald and Bolm have shown that copper in concentrations as low as 5 ppm is an effective catalyst for the coupling of iodo-benzene with amines, amides, phenols, and

Table 3. Results of ICP-MS Ruthenium Trace Analysis of 316SS Reactor Material and Inorganic Precipitates Isolated from Aqueous Acidic Reaction Mixtures

entry	sample[a]	Ru found [ppb][c]	detection limit [ppb]	quantification limit [±ppb]
1	Blank	<3	3	n.d.
2	Method Validation[b]	55000	450	1200
3	Reactor Steel exposed	<3	2	130
4	Reactor Steel not exposed	1400	52	3700
5	Precipitate 1	270	39	100
6	Precipitate 2	230	13	33

[a] All samples were prepared by digestion in *aqua regia*. [b] 0.00623 g of sample $RuCl_3 \cdot H_20$ (MW 261 g/mol) was digested in *aqua regia* and brought up to a final volume of 50 mL. By calculation the final concentration of Ru in this solution is 48.2 ug/mL (ppm). Ru recovery was 114%. [c] Re, Pd, Pt, Rh, Ir, or Au were not detected in any samples.

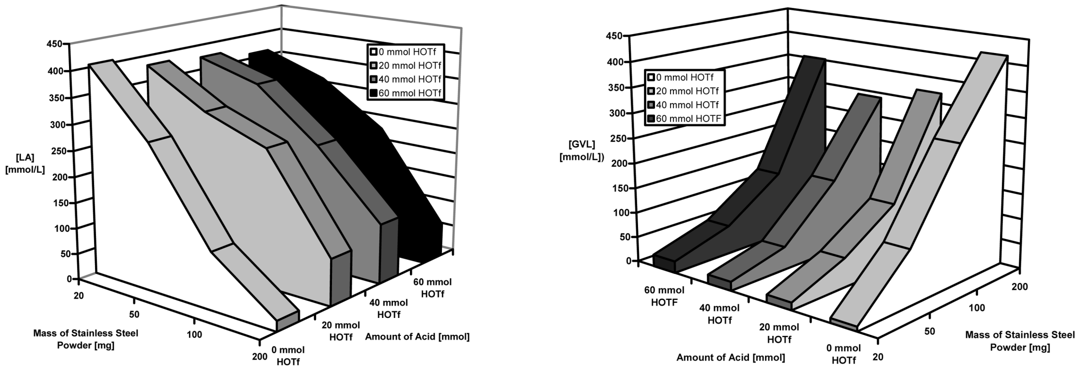

Figure 7. Consumption of levulinic acid and production of γ-valerolactone as a function of added 316SS powder (−325 mesh) as a catalyst and acid concentration. Reaction conditions: Levulinic acid [500 mmol/L], 800 psi $H_2(g)$ (initial pressure at ambient temperature), dimethylsulfone (ISTD) [100 mmol/L], in water, time = 24 h.

thiols.[51] We therefore also analyzed representative samples of the precipitates obtained as well as the stainless steel of the reactor body itself by ICP-MS.[52] Two stainless steel samples from one of the two 50 mL mini-reactors (Autoclave Engineers), one from the surface of the reactor steel that had been exposed to the reaction solutions during several hundred reactions with homogeneous ruthenium catalysts and one "virgin" steel sample obtained by machining filings from the unexposed interior of the material, as well as two typical green precipitates (Figure 6) from different reactions (glycerol deoxygenations) were dissolved in *aqua regia* and analyzed against a dilution series of a commercially available standardized solution containing Te, Re, Ru, Rh, Ir, Pd, Pt, and Au. The ICP-MS method was validated by dissolving a known amount of $RuCl_3 \cdot nH_2O$ in *aqua regia*, which led to full recovery of the ruthenium content. By inductively coupled plasma optical emission spectroscopy (ICP-OES) no evidence for the presence of another hydrogenating metal (Re, Rh, Ir, Pd, Pt) was found. In addition other previous studies, in which stainless steel samples were analyzed by inductively coupled plasma mass spectrometry (ICP-MS) (stainless steel needles used in blood-sampling) and imaging microprobe secondary ion mass spectrometry (stainless steel tubing) at very low detection limits also did not identify any traces of Re, Rh, Ir, Pd, or Pt,[53,54] that is, catalytic activity caused by an intrinsic contamination of 316SS by these metals originating from their ores and carried through the standard metallurgical process used in the manufacturing of the pure metals and ultimately the 316SS alloy is not an issue.

Table 3 lists the result of the ICP-MS analyses suggesting the presence of ruthenium in the samples at very low levels. However, at least for the stainless steel samples, the method is also susceptible to some possible interference for both the ^{99}Ru and ^{101}Ru isotopes by nickel. Since there is chloride in the digest, interference from NiCl (64 + 35 = 99) and NiCl (62 + 37 = 99) on the ^{99}Ru isotope and NiCl (64 + 37 = 101) on the ^{101}Ru mass may be responsible for the detection of low levels of ruthenium. Interference from argon from the plasma NiAr (61 + 38) on ^{99}Ru and NiAr (61 + 40) on ^{101}Ru may also take place. Using hydrogen as the collision/reaction gas we were able to minimize the effects of these interferences but probably not completely remove them. Repeating the analyses using larger sample sizes of stainless steel, resulted in better detection limits but also introduced more nickel into the system, which in turn led to larger limit of quantification limits on the basis of the above interferences. The fact that more ruthenium was found in the nonexposed reactor steel (Entry 4, Table 3) than in the exposed reactor steel (Entry 3, Table 3), which is the opposite of what would be expected, if ruthenium impregnated into the stainless steel were responsible for the observed catalytic activity,[55] further illustrates the limitations of the ICP-MS method in this particular analysis.

Conclusive evidence for the activation and catalytic activity of 316SS under aqueous acidic conditions comes from the series of experiments represented by Figure 7 using the general reaction conditions for the hydrogenation of LA as defined in Table 2, but with the addition of 316SS powder (−325 mesh), which substantially increases the stainless steel surface exposed to the reaction mixture. For example, for an addition of 200 mg 316SS powder the stainless steel surface adds ∼36 cm^2 of area (assuming perfectly spherical particles as the lower limit of surface area) to an estimated surface area of ∼90 cm^2 for the 50 mL reactor body including drive shaft, impeller, and lid alone.[56]

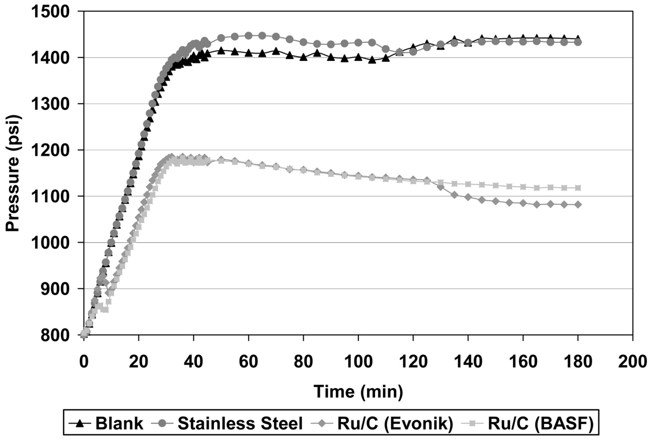

Figure 8. Hydrogen pressure vs time (180 min.) in the hydrogenation of LA in water as a function of catalyst employed. Reaction conditions: Levulinic Acid [500 mmol/L], dimethylsulfone (ISTD) [100 mmol/L], HOTf [40 mmol/L], no cat./2.50 g 316SS powder/0.250 g 5% Ru/C, 800 psi H_2 (initial pressure at ambient temperature), 250 °C.

For the same series of reactions, all of which also generate the green to brown precipitates shown in Figures 4 and 6, the graphs show the conversion of LA (left) and production of the primary hydrogenation product GVL (right) as a function of the amount 316SS powder (−325 mesh) and acid (HOTf) added to the reaction mixture. At the 24 h time point there is a clear increase of observed catalytic activity with increasing amounts of 316SS powder (0, 20, 50, 100, 200 mg) added proving that the 316SS must be catalytic active. This is true for any acid concentration (0, 20, 40, 60 mmol/L) tested, but the activity dependence on the amount of acid added plotted as the second dimension of the graphs does not follow a similar simple trend. The highest amount of GVL is obtained with no HOTf acid at all added, that is, LA itself is acidic enough to activate the steel for hydrogenation to GVL. However, Figure 7 does not plot the concentration of the secondary and tertiary deoxygenation products (PA, MT, PO, BE/BU) that complete the mass balances for these reactions and that require higher acid concentrations to be formed, but may be preferentially hydrogenated over the more stable GVL once present. The higher amounts of LA and lower amounts of GVL obtained with increasing acid concentration therefore reflect the complexity of the overall reaction cascade for LA deoxygenation (Scheme 2) and not the true impact of acid concentration on activity.

Comparison of Activated 316SS vs Ru/C As a Hydrogenation Catalyst. To assess the actual viability of 316SS as a hydrogenation/deoxygenation catalyst we compared its activity against two commercially available Ru/C catalysts (Evonik and ESCAT-BASF) at the arbitrary mass ratio of 10:1, that is, 2.50 g of −325 mesh 316SS powder vs 0.25 g of 5% Ru/C as added catalyst against LA.[57] The Ru/C catalyst where selected on the basis of their known activity on LA and resistance to aggressive aqueous media.[32,41] In these reactions the estimated total surface area of the added 316SS powder is ~427 cm^2, but the nature and number of actual active sites on this surface under the reaction conditions, that is, after etching by the aqueous acidic medium in situ, is unknown. A set of four reactions were performed for this comparison: one blank reaction, in which only the reactor body is catalytically active, one reaction with the addition of 316SS powder, and one each with the two commercial Ru/C catalysts. Figure 8 shows the pressure evolution in the reactor (50 mL Autoclave Engineers minireactor with 25 mL reaction solution 500 mmol/L LA) as a function of time (and inherently temperature for the initial 30 min heating phase) for 3 h. In this plot, the lower the recorded pressure in the sealed reactor the higher the amount $H_2(g)$ consumed and correspondingly the higher the relative catalysts activity. As is evident from this plot, at the catalyst loading chosen, the Ru/C catalysts are substantially more active. An important feature of the Ru/C catalyst emerges from closer inspection of the first 20 min of the pressure plot. During this time the reactor still heats up to its target temperature, but as the "dip" at $t \approx 10$ min in the pressure plots of the two catalysts shows they are already active at temperatures as low as 120 °C. We attribute this feature to the rapid and facile hydrogenation and cyclization of LA to GVL starting the reaction sequence of Scheme 2. This is not observed for the other 316SS only catalyzed reactions, which with reference to Figure 3 require higher reaction temperatures to become active. After ~30 min, at which point the reactor has reached it target temperature (250 °C), both Ru/C catalyzed reactions reach a maximum pressure of only ~1180 psi compared to >1400 psi for the 316SS catalyzed reactions (Figure 8), indicating that most of the $H_2(g)$ uptake has already occurred during the heating. Over a longer time scale (1440 min.) the Ru/C reactions show a further exponential decrease of $H_2(g)$ pressure from a maximum of ~1180 psi to ~1100 ± 10 psi followed by a very slow continuing decrease over 24 h.[58] We attribute this behavior to the reaction sequence LA → GVL followed by the much slower transformations GVL → PA and the decarboxylation reactions GVL → BE and/or PA → BU (Scheme 2). The 316SS reactions only show a slow linear pressure drop from their 1400−1450 psi high, with the 316SS powder catalyzed reaction showing ~100 psi total. The differences in observed pressure and hence total hydrogen uptake are directly reflected in the product distributions observed after 24 h represented in Figure 9. In comparison to the blank reaction the 316SS powder catalyzed reaction shows higher conversions of LA to PA, but less of the intermediate GVL, in congruence with the earlier discussion of the data presented in Figure 7. Under the reaction conditions only the Ru/C catalyzed reactions give full conversion of LA to deoxygenated products

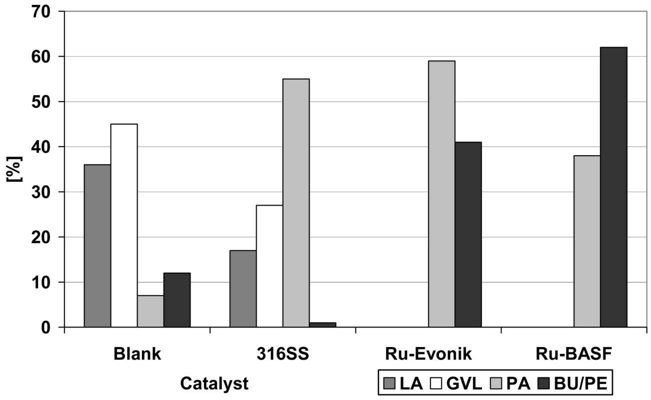

Figure 9. Product distribution in the deoxygenation of levulinic acid in water as a function of catalyst employed. LA = levulinic acid, GVL = γ-valerolactone, PA = pentanoic acid, BU/PE = 1-butene/butane for 316SS; butane/pentane (3:1) for Ru/C cat., determined by TCD-micro-GC against authentic standards. Reaction conditions: levulinic acid [500 mmol/L], dimethylsulfone (ISTD) [100 mmol/L], HOTf [40 mmol/L], no cat./2.50 g 316SS powder/0.250 g 5% Ru/C, 800 psi H_2 (initial pressure at ambient temperature), 250 °C, 24 h.

a) 316SS catalyst/reactor body

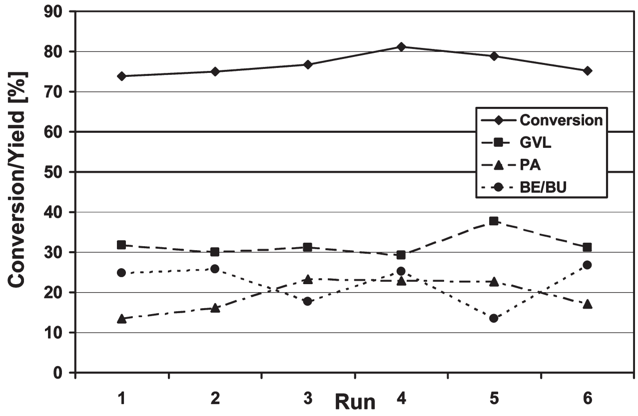

b) Ru/C (5 %) catalyst (EVONIK)

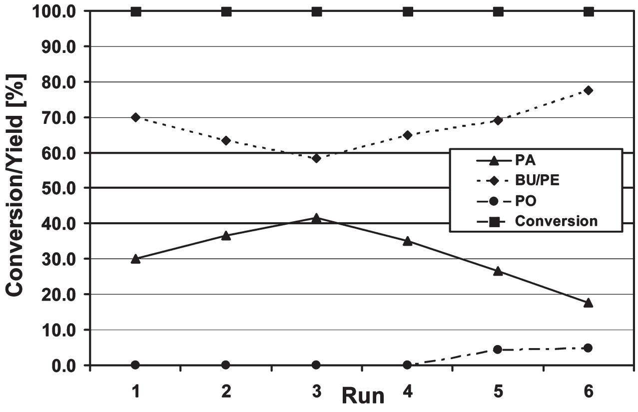

Figure 10. Effect of reuse of the (a) (top) 316SS powder vs the (b) (bottom) Ru/C (5%, EVONIK) catalyst on catalyst activity and product distribution. Reaction conditions: Levulinic acid [500 mmol/L], dimethylsulfone (ISTD) [100 mmol/L], HOTf [40 mmol/L], 2.5 g 316SS powder or 0.25 g Ru/C (5%, Evonik), 250 °C, 800 psi (initial pressure at ambient temperature), 12 h, water.

and generate 40—50% of total deoxygenation products, which by TCD-micro-GC analysis of gas samples taken from the head space of the reactor consist of a 3:1 mixture of BU and PE, but no BE.[59] The reaction with the 316SS powder generated almost as much PA as the Evonik catalyst, but much smaller amounts of total deoxygenation products in the gas phase, which as described above were again a mixture of BE and BU. For both catalyst types, the same product distributions are also observed when GVL rather than LA is used as the substrate.

A well recognized challenge in the deoxygenation of sugar or sugar alcohol derived substrates by heterogeneous catalysts is the fouling of the catalysts by the highly polar substrates through processes that effectively resemble the caramelization, that is, dehydration of sugar-derived polar substrates on an active and typically acidic catalyst surface, which, for example, led Shell to develop a two-step process for the deoxygenation of LA to PA that physically separates the reactions LA → GVL and GVL → PA using a nonacidic catalyst for the first and an acidic catalyst for the second step.[28,29] This avoids the formation of AL and pentenoic acid, which are known to cause catalyst fouling through polymerization. We therefore also carried out a series of experiments reusing both the 316SS powder as well as the Ru/C (EVONIK) catalyst six times under the same reaction conditions previously employed. Starting from 2.5 g for the stainless steel and 250 mg for the Ru/C catalysts, the mass loss of the 316SS powder was 147 mg after the first run and between 30 and 60 mg for the subsequent runs reflecting the etching process described above and less than 10 mg for the Ru/C catalyst, which for the latter is within the error range of the recovery, drying, and weighing procedure. For this study the reactors were not polished between runs to avoid loss of traces of catalyst still adherent to the reactor body. The results of the experiments are summarized in Figure 10. Both catalysts achieve consistent conversions: ~75% for the 316SS and quantitative for the Ru/C catalyst, that is, they do not show a decrease in activity per se. However, for the Ru/C the selectivity of the catalyst for PA vs total deoxygenation to a mixture of butane and pentane decreases (after a smaller initial increase) with repeated use, eventually reaching the same level (~ 18%) as the 316SS (albeit at higher conversion and therefore yield than the steel catalyst). The monotonous decrease in selectivity over the last four data points in the curve in Figure 10 b, suggests that this trend would continue over extended reuse, ultimately only yielding the total deoxygenation products. The selectivities of the 316SS catalyst show some variability over the six runs that do not follow a clear trend, but average out to ~30% GVL, ~ 25% BE/BU, and ~18% PA.

■ DISCUSSION

The sum of the experimental results presented above and in particular the fact that reactors never contacted with hydrogenating metals in either homo- or heterogeneous form are active and that the catalytic activity directly scales with the amount of 316SS powder added provides conclusive evidence that under aqueous acidic reducing conditions, that is, hydrogen atmosphere, as by necessity encountered in the deoxygenation of biomass, stainless steel is activated to form an active hydrogenation catalyst. While by ICP-MS there are possibly minute traces of ruthenium present in the reactions (<0.3 ppm), these are likely caused by the possible interferences discussed above or, if in fact real, would in our interpretation be too low to have catalytic significance. Also taking into account the error ranges (Quantification Limits, Table 3), effectively no ruthenium is present in the stainless steel samples. Furthermore if ruthenium deposits in the reactor body were responsible for the observed catalytic activity, they should also be active in sulfolane solution, but all control reactions in this solvent showed no or only marginal conversion ($\ll 5\%$).

The prevalence of dissolved chromium or precipitated chromium oxides in the reaction solutions suggests that the observed catalytic activity is in fact intrinsic to the 316SS with the mechanism of activation being an aqueous acid mediated etching of the protective chromium oxide layer (and possibly some nickel and iron oxides) exposing a surface of 316SS alloy in oxidation state zero. Under the reducing conditions the oxide layer is then not reformed until the reactor is opened to air at the end of the reaction, and the process repeats itself during the next reaction.[60,61] A conceivable mechanism for dissolution of the oxide layer under aqueous acidic conditions is pitting[62] occurring around manganese sulphide inclusions present in the stainless steel as demonstrated by Ryan et al.[63]

Once the oxide layer has been corroded away from the steel surface, the most likely active metal for hydrogenation is Ni; however, it can be speculated that synergistic effects between Fe, Ni, and Cr may be significant for the observed catalytic activity that possibly involves hydrogen spillover effects between sites that activate $H_2(g)$ and sites that are responsible for the actual hydrogenation steps.[10] While 316SS has a substantially lower activity than the two commercial Ru/C hydrogenation catalysts (and by extension likely other standard heterogeneous hydrogenation catalysts based on Ni, Pd or Pt), our observations may also open opportunities for a deliberate design of reactors with maximized wetted surfaces that take advantage of 316SS not only as a building material but also as a potentially cheap and easily accessed catalyst. Also, our results with LA as the substrate hint that it may better sustain its long-term selectivity to products that retain some of the oxygen content of a biomass derived feed rather than yielding the total deoxygenation products (here BE/BU and PE), which under the reaction conditions (aqueous, acidic, hydrogen atmosphere) constitute the thermodynamic sink of the reaction cascade.

CONCLUSION

Under aqueous acidic conditions and elevated temperature, 316SS is activated becoming a promiscuous catalyst for the hydrogenation of both carbonyl to alcohols and alkenes to alkanes. The phenomenon is intrinsic to a Brønstedt acidic aqueous environment and therefore of high relevance to the deoxygenation of biomass derived water-soluble substrates in stainless steel pressure reactors.

EXPERIMENTAL SECTION

General Procedures. Commercially obtained reagents were used as received. 316SS powder samples (- 325 mesh) were obtained from ESPI metals (lot # E3546 and D98238A). 5% Ru/C catalysts (Evonik and ESCAT-BASF) were obtained from STREM Chemicals. High-pressure hydrogenation reactions were conducted with 25 mL reaction solutions in two identical Autoclave Engineers (AE) Mini-Reactors with a 50 mL stainless steel (316 SS) reactor vessel or with 100 mL reaction solutions in a 500 or 600 mL Parr reactor, respectively. All high-pressure experiments employed industrial grade hydrogen gas. Pressure vs time curves where recorded using a Setra C206 pressure transducer (accuracy ±1 psi) fitted to the reactors. GC analyses were carried out on a Varian 3800 using a 30 m Rtx-1701 column. Quantification was achieved through a three-level calibration against authentic samples, employing dimethylsulfone (DMS, 100 mmol/L) as an internal standard, for all liquid substrates and products. Repeated injection of the calibration solutions as analytical samples established an accuracy and reproducibility of the quantification of ±2%. Gas sample analysis was carried out using an SRI 8610C micro-GC with a TCD detector. Authentic gas calibration samples containing 1000 ppm of the C1−C6 alkanes and C2−C6 1-alkenes in helium were obtained from GRACE Davison Discovery Sciences. GC-MS analysis were carried out on a Varian Saturn 2000 GC/MS employing a 30 m Rtx-1701 column running in default EI mode. HPLC analysis was carried out according to Varian Application Note 1534 (00.1 N H_2SO_4 on Metacarb 87H) using an RI Detector. SEM-XRF of isolated inorganic precipitates and ICP-OES trace analysis for platinum group metals and ICP-MS confirmation for ruthenium in the 316SS and chromium oxide precipitate samples were carried out by the University of Guelph Laboratory Services Division (an ISO 9001:2000 registered and SCS/GLP certified facility) using a NIST traceable precious metals standard solution in HCl (CMS-2 as supplied by Inorganic Ventures). Further details on the ICP-MS instrument parameters and method used are given in the Supporting Information.

Hydrogenation Experiments. In a typical deoxygenation experiment 25 mL of solution of substrates (500 mmol/L of glycerol or levulinic acid) and internal standard (dimethyl sulfone; 100 mmol/L) in water were dispensed into the 50 mL Autoclave Engineers minireactor. The appropriate amounts of catalyst and/or HOTf were added (the latter using a microliter syringe) and the reactor sealed. Using a manifold, the reactor was then evacuated using an aspirator pump (p_{min} = 16 Torr). The reactor was then pressurized to 800 psi with $H_2(g)$ and vented three times followed by a final pressurization to 800 psi. The reaction was started by switching on the heating mantle (defining t = 0 min.). The maximum reaction temperature of 250 °C was reached within 30 min for all reactors employed. For some reactions the reaction pressure was monitored as a function of time using a Setra C206 pressure transducer fitted to the reactor. At the end of the reaction (24 h), the reactors was cooled to room-temperature and then with an ice-bath (0 °C). While venting the reactor to ambient pressure, a gas sample from the head a space of the reactor was captured using a balloon and analyzed by GC-MS and micro-GC-TCD. Liquid samples obtained from the reaction solution were analyzed by GC and GC-MS as indicated above. Precipitates formed in the reaction mixtures were isolated by centrifugation and then dried at 110 °C before SEM-XRF and ICP-MS analysis.

ASSOCIATED CONTENT

Ⓢ **Supporting Information.** Images of micro-GC traces, GC-MS traces and spectra of gas samples taken from the head space of the pressure reactor proving the presence of 1-butene, butane, and pentane in the reaction mixtures. Material analysis sheets of the 316SS used to construct the two 50 mL Autoclave Engineers pressure reactors. ICP-MS instrument parameters and methods. Calculation of the total surface area of 316SS powder added reaction. (13 pages). This material is available free of charge via the Internet at http://pubs.acs.org.

AUTHOR INFORMATION

Corresponding Author

*E-mail: mschlaf@uoguelph.ca.

Funding Sources

The authors thank the Ontario Ministry of Agriculture, Food and Rural Affairs (OMAFRA) and NSERC Canada for funding

REFERENCES

(1) Dumesic, J. A.; Simonetti, D. A.; Kunkes, E. L. Patent WO 2009/129019 A2, 2009.

(2) Kunkes, E. L.; Simonetti, D. A.; West, R. M.; Serrano-Ruiz, J. C.; Gartner, C. A.; Dumesic, J. A. *Science* **2008**, 1159210.

(3) Huber, G. W.; Chheda, J. N.; Barrett, C. J.; Dumesic, J. A. *Science* **2005**, *308*, 1446.

(4) Dumesic, J. A.; Roman-Leshkov, Y. Patent WO 2008/151178 A1, 2008.

(5) Cortright, R. D.; Dumesic, J. A. Patent WO 2004/039918 A2, 2004.

(6) Dumesic, J. A.; Roman-Leshkov, Y.; Chedda, J. N. Patent WO 2007/146636 A1, 2007.

(7) Mehdi, H.; Fábos, V.; Tuba, R.; Bodor, A.; Mika, L. T.; Horváth, I. T. *Top. Catal.* **2008**, *48*, 49.

(8) Geilen, F. M. A.; Engendahl, B.; Harwardt, A.; Marquardt, W.; Klankermayer, J.; Leitner, W. *Angew.Chem., Int. Ed.* **2010**, *49*, 5510.

(9) Julis, J.; Holscher, M.; Leitner, W. *Green Chem.* **2010**, *12*, 1634.

(10) Deutschmann, O.; Knözinger, H.; Kochloefl, K.; Turek, T. In *Ullmann's Encyclopedia of Industrial Chemistry*; Wiley-VCH Verlag GmbH & Co. KGaA: Weinheim, Germany, 2009.

(11) Dykeman, R. R.; Luska, K. L.; Thibault, M. E.; Jones, M. D.; Schlaf, M.; Khanfar, M.; Taylor, N. J.; Britten, J. F.; Harrington, L. *J. Mol. Catal. A: Chem.* **2007**, *277*, 233.

(12) Gräfen, H. In *Ullmann's Encyclopedia of Industrial Chemistry*; Wiley-VCH Verlag GmbH & Co. KGaA: : Weinheim, Germany2000.

(13) Cerutti, L. *Int. J. Phil. Chem.* **1999**, *5*, 3.

(14) Ziegler, K. In *Adv. Organomet. Chem.*; Stone, F. G. A., West, R., Eds.; Academic Press Inc.: New York, 1968; Vol. 6, p 1.

(15) Layng, E. T. Hydrocarbon Research. U.S. Patent US 2506226, 1950.

(16) Shabtai, J. *Chem. Ind. (London, U. K.)* **1962**, 1282.

(17) Gornay, J.; Coniglio, L.; Billaud, F.; Wild, G. *J. Anal. Appl. Pyrolysis* **2010**, *87*, 78.

(18) Abbas, H. F.; Daud, W. *Appl. Catal., A* **2010**, *388*, 232.

(19) Loeker, F.; Leitner, W. *Chem.—Eur. J.* **2000**, *6*, 2011.

(20) Zhao, F. Y.; Ikushima, Y.; Arai, M. *Green Chem.* **2003**, *5*, 656.

(21) Zhao, F.; Ikushima, Y.; Arai, M. *Catal. Today* **2004**, *93*−*95*, 439.

(22) Taher, D.; Thibault, M. E.; Mondo, D. D.; Jennings, M.; Schlaf, M. *Chem.—Eur. J.* **2009**, 10132.

(23) Bozell, J. J.; Moens, L.; Elliott, D. C.; Wang, Y.; Neuenschwander, G. G.; Fitzpatrick, S. W.; Bilski, R. J.; Jarnefeld, J. L. *Resour. Conserv. Recycl.* **2000**, *28*, 227.

(24) *Top Value Added Chemicals from Biomass*; Werpy, T.; Peterson, G., Eds.; Pacific Northwest National Laboratory (PNNL), National Renewable Energy Laboratory (NREL), U.S. Department of Energy; 2004.

(25) Manzer, L. E. Patent WO 2003042201 A1, 2003.

(26) Manzer, L. E. Patent WO 2003042200 A1, 2003.

(27) Elliott, D. C.; Frye, J. G.; U.S. Patent 5,883,266, 1999.

(28) Lange, J.-P.; Shell; Patent WO 2009/007391 A1, 2009.

(29) Ayoub, P. M.; Lange, J.-P.; ; Patent WO 2008/1421272008.

(30) Brink, P. J. v. d.; Hebel, K. L. v.; Lange, J.-P.; Petrus, L.; ; Patent WO 2006/067171 A1, 2006.

(31) Palkovits, R. *Angew. Chem., Int. Ed.* **2010**, *49*, 4336.

(32) Lange, J.-P.; Price, R.; Ayoub, P. M.; Louis, J.; Petrus, L.; Clarke, L.; Gosselink, H. *Angew. Chem., Int. Ed.* **2010**, *49*, 4479.

(33) With these HPLC conditions the lowest molecular weight conceivable liquid product *n*-propanol has the highest retention time.

(34) See Supporting Information, Figure S1 for an image of the micro-GC trace.

(35) In this study GC-MS of gas phase samples detected mixtures of propene and propane after 3 h and pure propane after 24 h.

(36) Schuette, H. A.; Thomas, R. W. *J. Am. Chem. Soc.* **1930**, *52*, 3010.

(37) Hayashi, I.; Nogoro, E.; Hachihama, Y. *Nippon Kagaku Kaishi, Ind. Chem. Sect.* **1954**, *57*, 67.

(38) Horváth, I.; Mehdi, H.; Fábos, V.; Mika, L. T. *Green Chem.* **2008**, *10*, 238.

(39) Deng, L.; Li, J.; Lai, D. M.; Fu, Y.; Guo, Q. X. *Angew.Chem. Int. Ed.* **2009**, *48*, 6529.

(40) Heeres, H.; Handana, R.; Chunai, D.; Rasrendra, C. B.; Girisuta, B.; Heeres, H. J. *Green Chem.* **2009**, *11*, 1247.

(41) Yan, Z. P.; Lin, L.; Liu, S. J. *Energy Fuels* **2009**, *23*, 3853.

(42) Serrano-Ruiz, J. C.; Wang, D.; Dumesic, J. A. *Green Chem.* **2010**, *12*, 574.

(43) Remarkably this very old reaction is also claimed in a recent patent by DuPont (WO/2002/074760), the first claim of which reads "A process for preparing 5-methylbutyrolactone comprising heating levulinic acid in the presence of hydrogen and a catalytic amount of a metal catalyst, said metal catalyst having both a hydrogenation and a ring-closing function."

(44) See Supporting Information, Figure S2 for an image of the GC-MS trace and spectrum of this sample identifying/suggesting pentene as the product by comparison to an authentic sample of *n*-pentane.

(45) See Supporting Information, Figure S3 for images of the TCD-micro-GC traces obtained.

(46) Bond, J. Q.; Alonso, D. M.; West, R. M.; Dumesic, J. A. *Langmuir* **2010**, *26*, 16291.

(47) Neither reactor had previously ever been exposed to any other hydrogenating metal such as Re, Pd, Pt, Rh, or Ir.

(48) In this context the authors would like to debunk the common myth that the use of a glass or Teflon liner is sufficient to prevent the reactor from playing a role in catalytic processes, as this does not limit exposure of the reaction solution to the lid, drive shaft and impeller used to stir the reaction, all of which are typically constructed from the same material as the reactor body itself. This is particular true at high stirring speeds used when gaseous reactants must be dissolved in the reaction mixture or at high temperature, when substantial mass transport by convection and distillation takes place within the enclosed reactor space.

(49) The original analysis sheets of the 316SS used to construct the reactor as supplied by Autoclave Engineers are contained in the Supporting Information.

(50) Svehla, G. *Vogel's Qualitative Inorganic Analysis*, 7th ed.; Longman: Harlow, 1996.

(51) Buchwald, S. L.; Bolm, C. *Angew. Chem., Int. Ed.* **2009**, *48*, 5586.

(52) The drive shaft of the reactor impeller was sacrificed for this purpose.

(53) Paudyn, A.; Templeton, D. M.; Baines, A. D. *Sci. Total Environ.* **1989**, *89*, 343.

(54) Salaita, G. N. *Appl. Surf. Sci.* **1995**, *90*, 465.

(55) Note that the reactor surfaces were sandblasted and machine polished before each control experiment.

(56) See Supporting Information for a detailed calculation.

(57) These experiments were carried out in the same reactors, but after the trace analysis for ruthenium and 316SS powder experiments described above.

(58) See Supporting Information, Figure S4 for a replot of the same data as in Figure 8 over the extended time scale.

(59) See the Supporting Information, Figure S5 for the micro-GC traces of the gas samples.

(60) Stefanov, P.; Stoychev, D.; Stoycheva, M.; Marinova, T. *Mater. Chem. Phys.* **2000**, *65*, 212.

(61) The high susceptibility of 316SS to corrosion in nonoxidizing environments is a known issue, in particular in marine environments.

(62) Gräfen, H.; Horn, E.-M.; Schlecker, H.; Schindler, H. *Corrosion*; Wiley-VCH Verlag GmbH & Co. KGaA: Weinheim, Germany, 2000.

(63) Ryan, M. P.; Williams, D. E.; Chater, R. J.; Hutton, B. M.; McPhail, D. S. *Nature* **2002**, *415*, 770.